



# Magnesium Sulfate ( $\text{MgSO}_4$ ) Attack and Chloride Isothermal Effects on the Self-consolidating Concrete Containing Metakaolin and Zeolite

Kianoosh Samimi<sup>1</sup> · Ali Akbar Shirzadi Javid<sup>2</sup>

Received: 21 September 2018 / Accepted: 23 March 2020 / Published online: 11 April 2020  
© Shiraz University 2020

## Abstract

The aim of this study is to investigate the mechanical and durability properties of the self-consolidating concrete (SCC) containing fine sand as filler and two types of pozzolan including metakaolin and zeolite. The limestone filler of the reference SCC is replaced by fine sand, and also partial substitution of 10% and 15% of ordinary Portland cement is replaced by metakaolin and zeolite. Also, sustainability in aggressive conditions like magnesium sulfate ( $\text{MgSO}_4$ ) as well as total, free and chloride binding concentration is evaluated. The results of physicochemical characterization showed that the used zeolite is clinoptilolite, which has a higher pozzolanic activity compared to the metakaolin. From this research, the SCC containing zeolite, despite the strong pozzolanic activity of zeolite, shows a low compressive strength (about two times) compared to the other SCCs. The results also showed that zeolite (optimum percent is 15%) enhanced resistance to the chloride ions penetration and resistance to  $\text{MgSO}_4$  attack, 1 and 5 times, respectively, compared to that in SCC with metakaolin.

**Keywords** Magnesium sulfate · Chloride isothermal effects · Self-consolidating concrete · Supplementary cementitious materials

## 1 Introduction

The sulfate attack and chloride penetration represent a significant challenge to the construction of marine structures. One of the problems encountered in the documentation of concrete durability is the question related to the definition of chloride ion penetration mechanism and magnesium sulfate attack.

Some visible examples of damage caused by reactions of concrete components with sulfates include scaling, delamination, macro-cracking and possibly the loss of cohesion. In many research papers, deterioration of concrete in sulfate environments is classified as two phenomena: chemical sulfate attack and physical sulfate attack (Neville 2004; Santhanam 2001; Maes et al. 2017). However, some researchers like to classify these sulfate attacks as internal and external,

respectively. Magnesium sulfate is very aggressive compared to sodium sulfate.

The formed hydrated magnesium silicate (M–S–H) does not have binding properties, and therefore, the hydrated paste becomes soft and incoherent (Tagnit-Hamou and Petrov 2000). For equivalent porosity, Anissa Bessa (2004) has shown that mortars based on cement CEM III/C have a higher chemical resistance than those based on cement CEM I. For a given type of cement, there is a strong correlation between the chemical resistance and the compressive strength, while the correlation with the porosity is comparatively very low (Anissa Bessa 2004). The chemical resistance is depended mostly to the nature and the quality of the bonds in the cement matrix. Indeed, the question of portlandite consumption is critical concerning sulfate attack. Ghrici et al. (2007) added that the formation of C–S–H gels leads to the densification of paste–granulate transition zone, which limits the diffusion of  $\text{SO}_4^{2-}$  ions.

Anissa Bessa (2004) and Tosun et al. (2009) found that the liaison contribution of mineral admixtures plays a structural role in cementitious matrix bonding from a mechanical point of view than a quantitative role in the reduction of porosity. In terms of durability, this structuring contribution translates to better resistance against severe chemical

✉ Kianoosh Samimi  
K\_samimi@sbu.ac.ir

<sup>1</sup> Faculty of Civil, Water and Environmental Engineering, Shahid Beheshti University, Tehran, Iran

<sup>2</sup> School of Civil Engineering, Iran University of Science and Technology, P.O. Box 16765-163, Narmak, Tehran, Iran

aggression. Hassan et al. (2013) who exposed SCC specimens to  $Mg_2SO_4$  for 118 days have shown that the addition of fly ash (FA), rice husk ash (RHA) and ground-granulated blast-furnace slag (GGBFS) can improve SCC resistance to magnesium sulfate attack. Karakurt and Topçu (2011) explained that ettringite formation in the microstructure of the mixture against sulfate attack was limited with the usage of zeolite. The results of Behfarnia and Farshadfar (2013) indicated that metakaolin and zeolite had better effects than silica fume on SCC durability to magnesium sulfate attack condition.

Another aggressive condition is placing concrete in the chloride condition or existing chloride ion in the concrete. The results of the study by Valipour et al. (2017) and Khoshroo et al. (2018a) indicated that the optimum replacement percentage for zeolite in concrete was in a range between 10 and 20% which means improvement in chloride penetration resistance as concrete durability in aggressive condition. The results of the article published by Tadayon et al. (2016) indicated similar effects on concrete durability in chlorine environments by replacing 10% natural zeolite, 5% metakaolin and 5% silica fume. Another study by Valipour et al. (2013) showed that, in general, zeolite is not as same as silica fume or metakaolin from the viewpoint of activity, although it could be used as an excellent replacing admixture because it has better durability characteristics and is economical. Sabet et al. (2013) expressed that using mineral admixtures generally improves durability characteristics of the concrete. However, silica fume is slightly better than natural zeolite or fly ash in this matter. Dousti et al. (2013) tried to evaluate the effects of admixtures from the viewpoint of energy. They showed that at the equal replacement percentage of 10%, the activation energy value of the mixture containing zeolite was higher than that of the mixture containing silica fume. However, the problem in this area is that the produced chloride in concrete in two forms: free chloride and bounding chloride (Zhang et al. 2018).

This paper investigates and compares the effect of fine sand as filler and two different pozzolans (metakaolin and zeolite) on compressive strength and chemical resistance of SCC. The impact on the resistance to chloride penetration is also investigated. For this purpose, first, the chemical and mineralogical composition, as well as the microstructure of two pozzolans, was studied. After this, hydration analysis was realized by the progress of evaporable water, and non-evaporable water content in cement paste blended with supplementary cementitious materials and also pozzolanicity of two pozzolans examined by Chapelle test. The tests concerning the chemical resistance were also performed in order to evaluate the durability properties with time, including magnesium sulfate attack. Finally, the resistance to chloride penetration of the different mixtures was evaluated by the determination of free, binding and total chloride concentration.

## 2 Experimental Program

### 2.1 Materials and Mix Proportion

The constant Portland cement type II content ( $450 \text{ kg/m}^3$ ), water-to-cementitious materials ratio of 0.4 and gravel-to-sand ratio of  $G/S = 1$  were considered for the preparation of concrete mixtures. Two concrete mixtures based on Portland cement, SCCL and SCCS contain limestone powder and fine sand as filler, respectively. The SCC by limestone powder (SCCL) was considered as a reference concrete. In the other four formulations with limestone filler, SCCM10, SCCM15, SCCZ10 and SCCZ15, metakaolin and zeolite were used as supplementary cementitious materials with two different substitute percentages of 10% and 15% by Portland cement. Portland cement with a specific gravity of  $3.15 \text{ g/cm}^3$  and a Blaine fineness of  $2900 \text{ cm}^2/\text{g}$ , in accordance with ASTM C150 2009, were consumed. The metakaolin used in this research has a specific surface area of  $3920 \text{ cm}^2/\text{g}$  and a specific gravity of  $2.49 \text{ g/cm}^3$ . The used zeolite as shown in Table 1 is a siliceous since it contains a high amount of Silica. It has a specific surface area of  $4060 \text{ cm}^2/\text{g}$  and a specific gravity of  $2.25 \text{ g/cm}^3$ . The chemical analysis, particle size distribution (PSD) of cementitious materials and aggregate grading curves are shown in Table 1 and Fig. 1, respectively.

For all mixtures, crushed angular material of 6–12 mm nominal size was used as a coarse aggregate (gravel), and natural sand with a maximum size of 4 mm used as a fine aggregate. A high-range water-reducing admixture (HRWRA) with a specific gravity of  $1.1 \text{ g/cm}^3$  based on modified polycarboxylate ether chains was also consumed. The dosage of superplasticizer is experimentally determined from tests on fresh concrete to obtain a slump flow diameter of  $700 \pm 20 \text{ mm}$  for all SCCs (Samimi et al. 2017, 2018a). Table 2 shows the mix proportions of the mixtures.

### 2.2 Microstructure Investigation of Powders

#### 2.2.1 SEM–EDS Analysis

Figures 2 and 3 present SEM images of limestone powder and fine sand filler as well as the corresponding chemical analysis respectively. As indicated, limestone filler is composed of small particles in comparison with sand filler. The main chemical elements present in limestone filler are C, Ca, Si, Al, Na elements. According to Fig. 3, the main chemical elements present in fine sand filler are Si, Al, Mg, Fe, Ca, K. Figure 4 illustrates SEM images of metakaolin powder with chemical analyses. Metakaolin appears to be composed of dense particles that resemble crystal

**Table 1** Chemical analysis of Portland cement type II, limestone powder, metakaolin and zeolite

Chemical analysis (% by mass)	Cement (type II)	Limestone powder	Sand filler	Metakaolin	Zeolite
Loss of ignition	1.3	42.88	7.11	0.78	11.94
SiO <sub>2</sub>	21.74	1.19	55.85	65.93	69.72
Al <sub>2</sub> O <sub>3</sub>	5.0	0.85	14.42	13.71	13.54
Fe <sub>2</sub> O <sub>3</sub>	4.0	0.3	7.01	0.23	1.26
CaO	63.04	48.82	9.5	5.46	0.87
MgO	2	1.58	2.83	3.84	2.45
SO <sub>3</sub>	2.3	–	0.08	–	–
CO <sub>2</sub>	–	–	5.70	–	–
CaSO <sub>4</sub>	–	–	0.14	–	–
Cl	–	–	–	–	–
Insoluble residue	0.60	–	–	–	–
Alkalis (Na <sub>2</sub> O% + 0.658K <sub>2</sub> O %)	1	–	–	–	–
Na <sub>2</sub> O + K <sub>2</sub> O	–	4.27	–	8.93	0.13
Free Cao	1.4	–	–	–	–
Humidity	–	0.11	–	0.1	0.09
C <sub>3</sub> S	45.5	–	–	–	–
C <sub>2</sub> S	28.0	–	–	–	–
C <sub>3</sub> A	6.5	–	–	–	–
C <sub>4</sub> AF	12.2	–	–	–	–

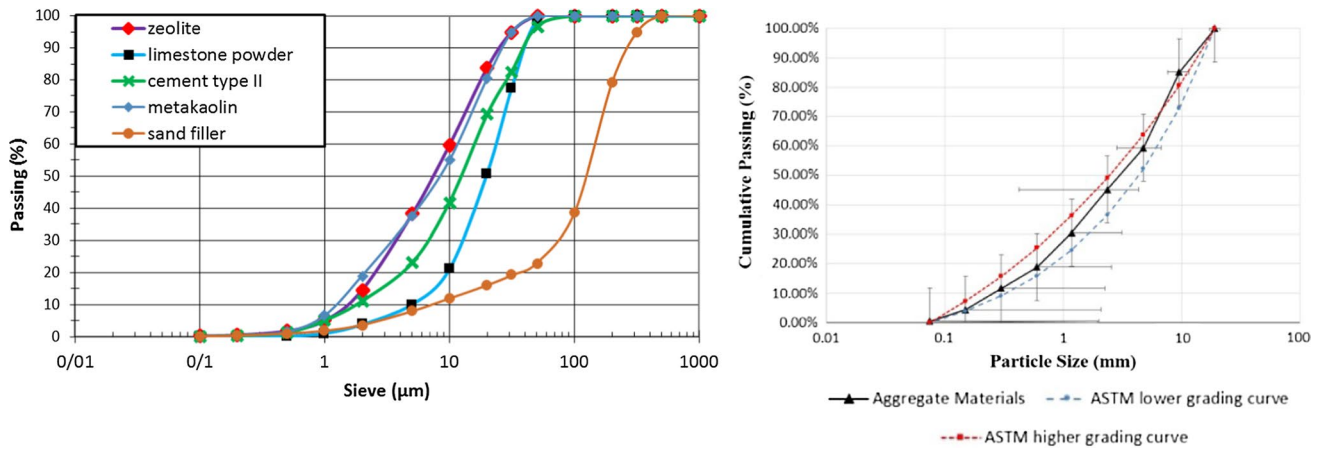


**Fig.1** Particle size distribution of materials; left: fine materials, right: aggregates

**Table 2** Mix proportions of SCC mixtures (kg/m<sup>3</sup>)

Mix name	Water (w)	Cement (c)	w/c <sub>m</sub>	Gravel	Sand	Limestone filler	Sand filler	Superplasticizer	Zeolite	Metakaolin
SCCL	180	450	0.4	790	790	150	–	4.85	–	–
SCCS	180	450	0.4	790	790	–	150	5.27	–	–
SCCM10	180	405	0.4	790	790	150	–	4.7	–	45
SCCM15	180	382.5	0.4	790	790	150	–	6.53	–	67.5
SCCZ10	180	405	0.4	790	790	150	–	8.94	45	–
SCCZ15	180	382.5	0.4	790	790	150	–	21.62	67.5	–

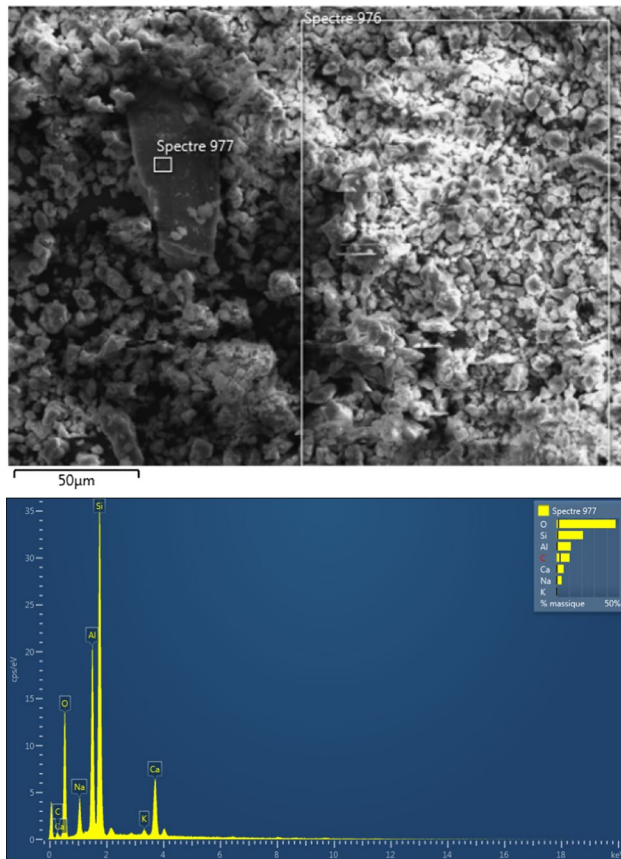


Fig.2 SEM images and chemical analysis of limestone filler

material containing the following chemical elements Si, Al, Ca, Fe, K. SEM images of zeolite powder with chemical analyses are shown in Fig. 5. Zeolite appears to be composed of small plate particles containing the following chemical elements Si, Al, Na, K, Fe, Ca, Na.

### 2.2.2 XRD Analysis

XRD results for metakaolin and zeolite pozzolan are illustrated in Fig. 6. XRD diffractogram of metakaolin showed that it is composed of anorthite and quartz minerals, which are siliceous natural metakaolin. XRD diffractogram of the studied zeolite corresponds to clinoptilolite which is one of the siliceous natural zeolites.

### 2.3 Casting and Curing

Cubic, cylindrical and prismatic samples were cast by ASTM C31 (2012) and ASTM C511 (2013) guidelines. After casting, samples were covered with two layers of plastic sheets and placed in temperature-controlled room at  $22 \pm 2$  °C for 24 h. All samples were demolded after 24 h and cured up to the age of testing in a saturated lime

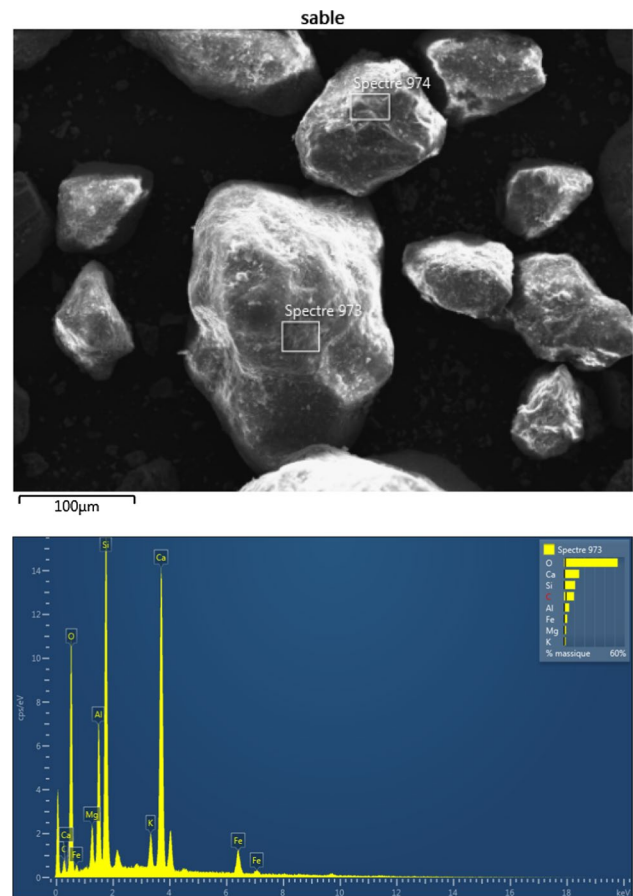


Fig.3 SEM images and chemical analysis of fine sand filler

solution to prevent possible leaching of  $\text{Ca}(\text{OH})_2$  from these specimens. The hardened concretes were tested for compressive strength, chemical resistance test as well as  $\text{MgSO}_4$  attack. Also, it was used for the determination of free, binding and total chloride penetration by diffusion in the non-steady state.

## 3 Test Method

### 3.1 Analysis by SEM–EDS and XRD

Scanning electron microscopy observations associated with elemental microanalysis by X-ray spectrometry were performed on limestone powder, sand filler and two pozzolans using a JSM 7100F SEM, equipped with an Oxford-based EDS SDD detector. Before analysis, the samples metalized with gold–palladium in order to make their surface conductive. XRD analysis was performed on metakaolin and zeolite using a Bruker D8 X-ray diffractometer with a monochromatic Cu source and a fast linear detector Lynx Eye.

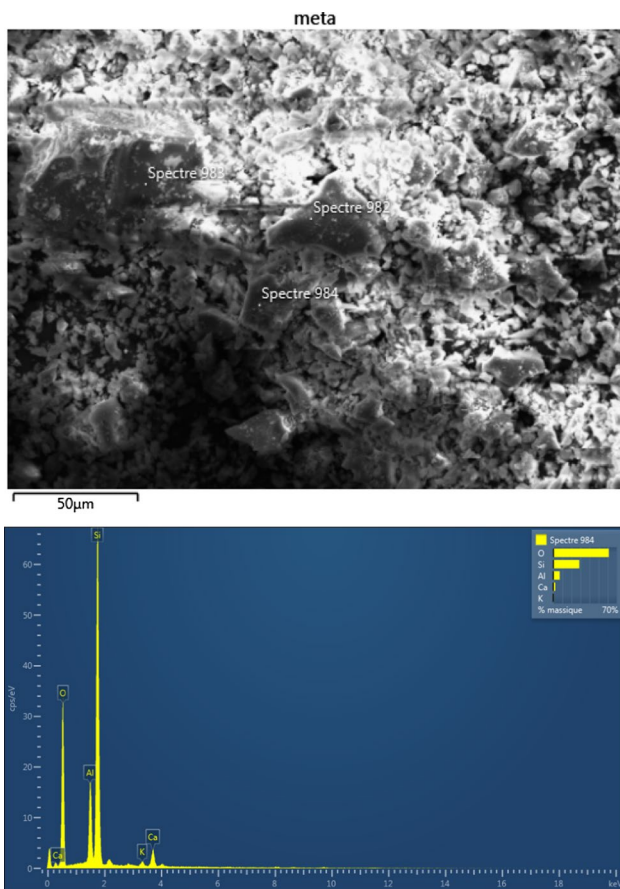


Fig.4 SEM images and chemical analysis of metakaolin powder

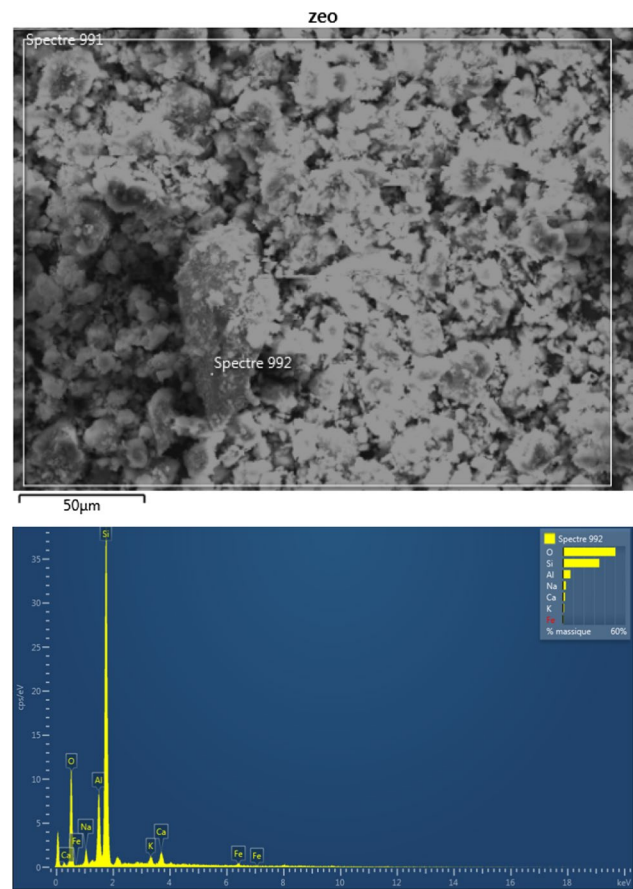


Fig.5 SEM images and chemical analysis of the studied zeolite

### 3.2 Hydration Analysis

#### 3.2.1 Evaporable and Non-evaporable Water Content Measurement

The evaporable water content corresponds to the mass loss of water between 105 and 20 °C (Eq. 1). Also, the non-evaporable water content corresponds to the mass loss of water between 1000 and 105 °C (Eq. 2) (Samimi et al. 2017). The measurements were carried out on binder pastes. The powders obtained were put in crucibles and placed in a furnace. The samples are carried in the ambient temperature to 1000 °C at a rate of 10 °C per minute and a bearing 20 h at 105 °C and 2 h at 1000 °C. The evaporable water content and non-evaporable water content at 105 °C are calculated by the following equations:

$$W_e = \frac{W_{20^\circ\text{C}} - W_{105^\circ\text{C}}}{W_{20^\circ\text{C}}} \quad (1)$$

$$W_{ne} \text{ at } 105^\circ\text{C} = \frac{W_{105^\circ\text{C}} - W_{1000^\circ\text{C}}}{W_{105^\circ\text{C}}} \quad (2)$$

where  $W_e$  is evaporable water content;  $W_{ne}$  is non-evaporable water content;  $W_{20^\circ\text{C}}$  is the mass in ambient air;  $W_{105^\circ\text{C}}$  is the mass of the sample after drying at 105 °C; and  $W_{1000^\circ\text{C}}$  is the mass of the sample after heating at 1000 °C.

#### 3.2.2 Pozzolanicity by Chapelle Test

In order to evaluate the pozzolanic activity of the studied metakaolin and zeolite, the measurements based on the modified Chapelle test are performed according to NF P18-513 (2012).

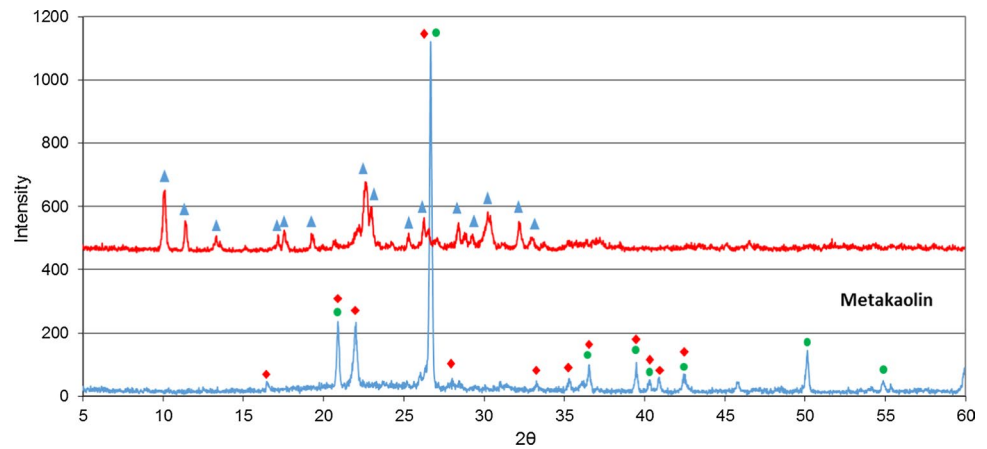
### 3.3 Compressive Strength

This test was done in accordance with BS 8110: part 1: 1997 for several ages as a young age and long-term conservation (1, 3, 7, 14, 28, 90, 180 and 365 days).

### 3.4 External Sulfate Attack Test

In the literature, there is no (until now) accelerated standardized test to examine the behavior of concrete samples concerning sulfate attack. For this procedure, concrete

**Fig.6** XRD analysis of metakaolin and zeolite pozzolan: anorthite, quartz and clinoptilolite



samples after reaching the age of 28 days of conservation in lime water were kept in two different conditions as a control condition (tap water) and sulfate medium. For magnesium sulfate solution, the concentration of 5% and the pH between 4 and 6 were considered. Samples were removed from solution weekly, cleaned with a paper towel and allowed to dry at 20 °C, and 50% RH for 30 min before weighing, and visual inspection. Six cubic samples ( $10 \times 10 \times 10 \text{ cm}^3$ ) are used per formulation for mass verification for 360 days of testing and to measure the compressive strength at maturity of 28, 90 and 360 days immersed in the sulfate solution (ASTM C 267, 1997). The percentage of all variations is calculated by the difference between original quantity of mass and compressive strength and their quantity after immersion in magnesium sulfate solution divided by the original quantity. Two prismatic samples ( $7.5 \times 7.5 \times 28.5 \text{ cm}^3$ ) are used per formulation for dimensional change verification according to standard ASTM C 1012-04. This step is performed every week for 4 months and after every three weeks until the end of the test. The measurements were carried out using a micrometer comparator with an accuracy of 0.001 mm regularly. The dimensional variation of each specimen is calculated from the following relation:

$$\Delta L = \frac{Lx - Li}{Lg} \times 100 \quad (3)$$

$\Delta L$  = change in length at age  $x$  (%).  $Lx$  = sample length read by comparator at age  $x$ .  $Li$  = sample length read by comparator before immersion.  $Lg$  = nominal length of the gauge.

A visual inspection was carried out by taking high-resolution photographs of corroded samples after 360 days of immersion. This method is useful for comparing the performance of samples to gain a better understanding of the corrosion rate and resistance of the different samples exposed to magnesium sulfate attack.

### 3.5 Chloride Ion Fixation by Diffusion in Non-steady State

ASTM C 1543-02 was used on three concrete specimens ( $\emptyset 100 \times 50 \text{ mm}$ ) per mix design with the aging of 90 days in order to characterize the chloride ions fixation by measurement of free, total and bounding chloride. The concrete specimens were maintained for 90 days in the saline solution containing 165 g/l of NaCl. In order to measure the free, bonding and total chloride concentration profile in the tested specimen, different 3-mm slices of concrete were cut from the surface. The dissolution and measurement of the free and total chlorides were obtained by the filtration of a solution of a powder product (almost 5 g) and distilled water. The chloride ion concentration was determined by adding the silver nitrate into the solution containing powder until the color red appears. This test is performed according to the standard AFREM, 1997. The following relation gives the content of free chlorides expressed in grams per 100 g of sample:

$$Cl = \frac{(35.5 \times C_{Ag} \times V_e \times V_p)}{(10 \times M_{pe} \times V_{fiol})} \quad (4)$$

The following relation gives the content of total chlorides expressed in grams per 100 g of sample:

$$Cl = \frac{(35.5 \times C_{Ag} \times V_e)}{(10 \times M_{pe})} \quad (5)$$

where  $C_{Ag}$  is the concentration of silver nitrate ( $\approx 0.01 \text{ M}$ ),  $V_e$  is the volume of silver nitrate,  $M_{pe}$  is the sampled 5 g of powder product,  $V_{fiol}$  is the volume of the filtrate solution up to 250 ml in a volumetric flask and  $V_p$  is the volume of the solution taken ( $\approx 50 \text{ ml}$ ) to mix with 2 ml concentrated nitric acid in order to acidify the medium and stabilize the chlorides in solution. Finally, the bounding chloride content is calculated by the difference between total chloride and free chloride.

## 4 Result and Discussion

### 4.1 Compressive Strength of SCC Mixtures

Figure 7 shows the strength rise of mixes based on the average strength of three samples tested at each age as a function of log (days). The most considerable resistance from 7 to 365 days is observed for the mixture containing metakaolin 15% (SCCM15). In contrast, the minimum resistance is belonged to the mixture containing zeolite 15% (SCCZ15) at all ages. The compressive strength in concrete containing 15% of metakaolin was 1.15, 1.24, 1.25, 1.2, 1.23, 1.19 and 1.17 times higher than the one of the control concrete at 3, 7, 14, 28, 90, 180 and 365 days of age, respectively. Use of metakaolin 15% had a very positive effect on the compressive strength from the age of 7 days compared to the other mixtures. This result is very consistent with the results given by Siddique and Klaus (2009). On the other hand, the magnitude of compressive strength in SCC containing 10% of metakaolin was closer to that in the control concrete until the age of 28 days. After 28 days of aging, the progress of the compressive strength in SCCM10 was more remarkable in comparison with the compressive strength in the control mix. The results match the experimental results of previous studies performed on SCC made by metakaolin at various percentage levels (Siddique and Klaus 2009; Alanazi et al. 2017; Hassan et al. 2012). The significant difference between metakaolin found in Iran existing in Europe has the  $\text{SiO}_2$  and  $\text{Al}_2\text{O}_3$  content. Indeed, metakaolin found in Iran contains more  $\text{SiO}_2$  (Table 1). Also, the compressive strength of concrete with metakaolin of Europe, during early age,

is less than that of the concrete mixture without addition. On the other hand, the Iranian metakaolin increases the compressive strength from an early age. This behavior difference has been well documented in the previous work by the first author, along within the research conducted by San Nicolas et al. (2014), Samimi et al. (2018b). On the contrary, zeolite had a negative impact on the ascending trend of the compressive strength according to the result illustrated in Fig. 7. As it is clear, the compressive strength of mixtures containing 10% and 15% of natural zeolite was lower than that of control concrete at all ages. Accordingly, it concludes that the use of zeolite as described here has a negative effect on compressive strength in SCC compared to that of the control concrete. These results are in good agreement with the experimental results of previous studies performed on SCC composite based on 15% of natural zeolite (Najimia et al. 2012).

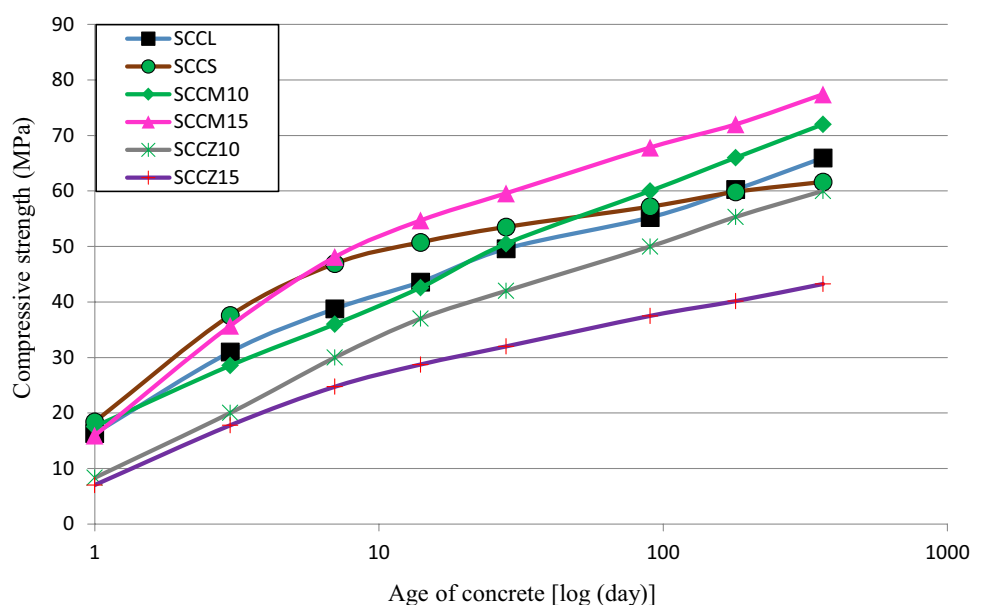
According to these results, a higher resistance development is noted with the use of sand filler. This is true up to 90 days of maturation, beyond which the resistance stabilizes for the concrete with sand filler, but it continues to increase for the SCC with limestone filler. The adhesion between the matrix and the calcareous grains may explain this, which improves with time. The highest resistance of 1–3 days and 7–365 days is obtained for SCCS and SCCM15, respectively.

### 4.2 Hydration Analysis

#### 4.2.1 The Course of Evaporable Water and Non-evaporable Water Content

The primary purpose of conducting thermal analysis is to measure the content of evaporable and non-evaporable

**Fig.7** The results of compressive strength of SCC mixtures with curing time



water at 105 °C. The amount of evaporable water can be linked to the porosity. The non-evaporable water is considered as an essential and reliable indicator of the hydration progress in the modification of microstructure. The results relating to the evaporable and non-evaporable water at 1, 3, 7, 14, 28, 90, 180 and 365 days of aging are displayed in Figs. 8 and 9, respectively. Increased non-evaporable water content over time was found, followed by a decrease in evaporable water for all formulations. This first observation is predictable due to the continued hydration of the binders. Further, paste with zeolite, even if it contains less cement and therefore less clinker, could yield non-evaporable water contents close to that of the control, which was observed to be more significant in the case of binders with zeolite 15% for all days of maturation. These

results suggest the presence of additional hydration which may be related to the pozzolanic activity and the formation of hydrates. Thus, the amount of evaporable water in the paste containing 15% metakaolin was less than that in the control mixture from 3 days of maturation. According to these results, the quantity of compressive strength and durability properties in mixture containing metakaolin and zeolite can be well justified at each curing time by considering the amount of evaporable and non-evaporable water, respectively. In the paste containing zeolite, the evaporable water content was higher compared to that in the control mix, particularly in the paste with 15% of zeolite (Fig. 8). This fact can be explained by the low mechanical behavior obtained with the mixture containing zeolite pozzolan. On the other hand, the tremendous non-evaporable water

**Fig.8** Evaporable water content in the studied mixtures at different ages

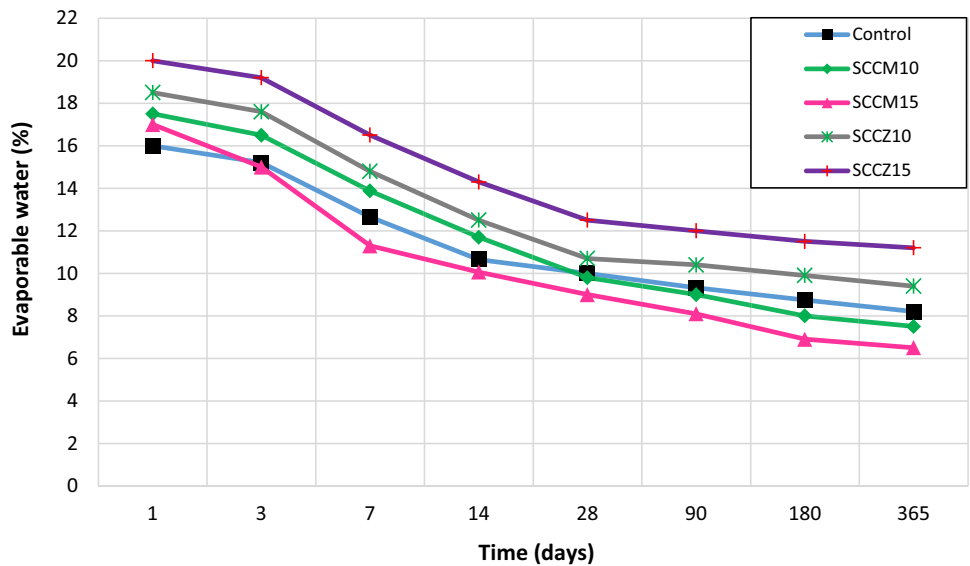
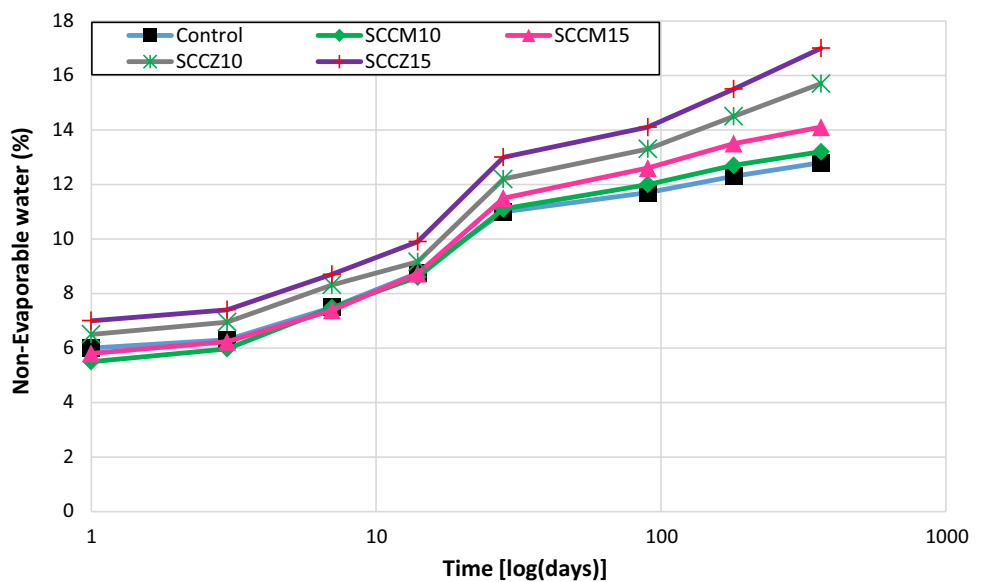


**Fig.9** Non-evaporable water content in the studied mixtures at different ages





content in the mixture containing zeolite can be associated with a high pozzolanic reaction.

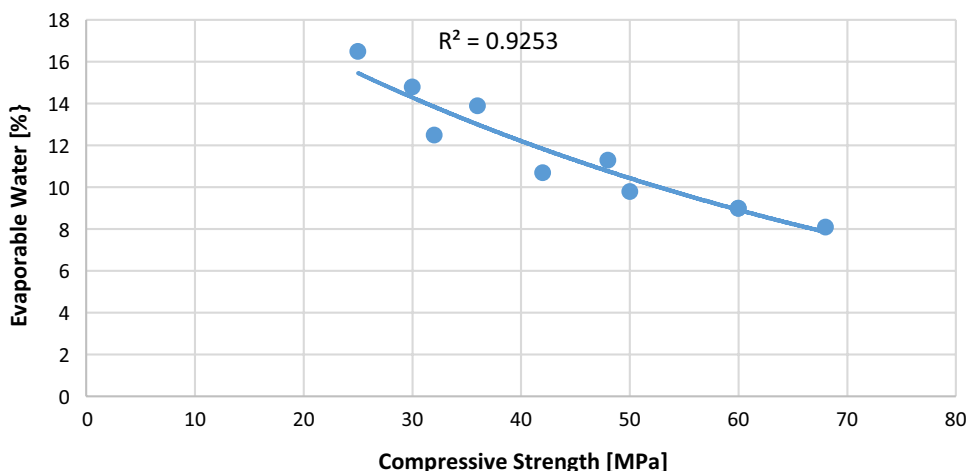
Determining the amount of calcium hydroxide fixed by metakaolin and zeolite according to the modified Chapelle test is a method of assessing its pozzolanic activity. The amount of  $\text{Ca}(\text{OH})_2$  fixed by metakaolin was taken as 380 mg, and the one for zeolite was equal to 490 mg. This result shows a higher pozzolanic reaction of zeolite compared to metakaolin which is in good agreement with those of non-evaporable measurements. Also, the relationship between the compressive strength of mixtures and evaporable water content is illustrated in Fig. 10. As can be seen, the elevation of compressive strength causes reduced evaporable water content of mixtures.

### 4.3 The Effect of $\text{MgSO}_4$ Attack

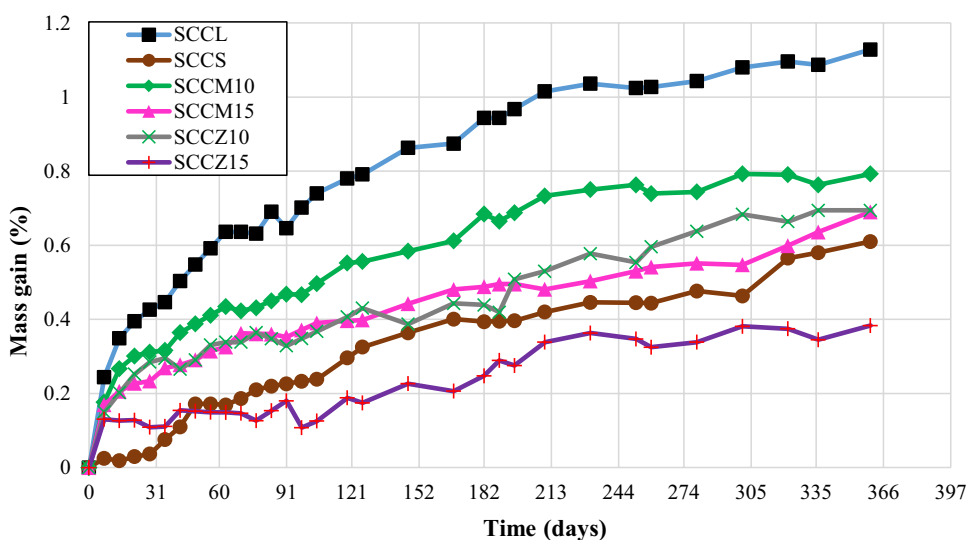
The mass variation of the samples immersed in the 5%  $\text{MgSO}_4$  solution as a function of immersion time is

illustrated in Fig. 11. This figure indicates the mass growth in all mixtures immersed in the  $\text{MgSO}_4$  solution during the immersion time. Viewing these characteristics, we cannot observe a visible degradation in all mixtures up to 365 days of immersion. This effect suggests that degradation by external magnesium sulfate attack is slower and the mass loss that it will probably be visible after this immersion time. This progress is due to the continuity of hydrates in different SCCs and the formation of gypsum and secondary ettringite. The reason for mass growth in all mixtures is also related to two reasons, including filling cracks with water and the participation of water in the process of hydration of ettringite. This fact is entirely congruent with the approach given by Hocine Siad (2015). From Fig. 11, there is a more noticeable difference in the mass gain between SCC containing sand filler (SCCS) and control SCC (SCCL). This fact may be justified by the type of existent filler in SCCL and SCCS. The abundant amount of calcium carbonate present in the limestone filler compared to that in sand filler can influence

**Fig.10** The relationship between compressive strength of mixtures and evaporable water content



**Fig.11** Mass variation of all SCCs immersed in the  $\text{MgSO}_4$  solution



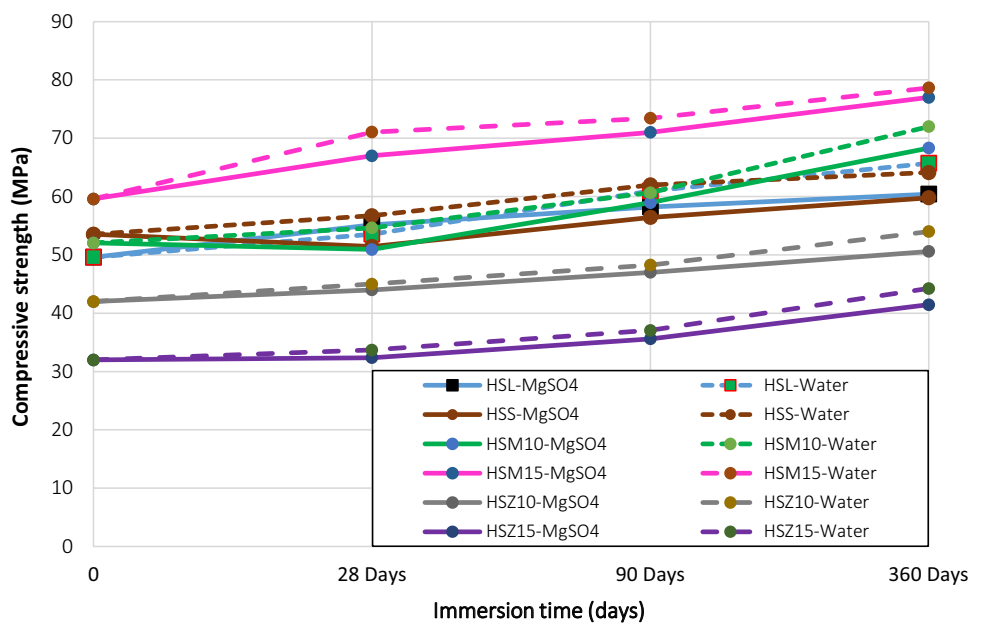
the increase of mass gain in SCCL compared to that in SCCS since gypsum is produced more in SCCL. According to our results, relative to the mass growth, the use of sand filler, metakaolin and zeolite can be beneficial in lowering mass variation of concrete exposed to the external attack by magnesium sulfate. The latter is more pronounced where the rate of replacement of pozzolan increases.

Figure 12 presents the progress of the compressive strength concerning the samples immersed in a sulfate medium and a control medium. The analysis of the results illustrated in Fig. 12 shows that the compressive strength of all mixtures preserved in the sulfate solution develops positively at all times of immersion except for SCCS and SCCM10 at the age of 28 days of immersion. After 28 days

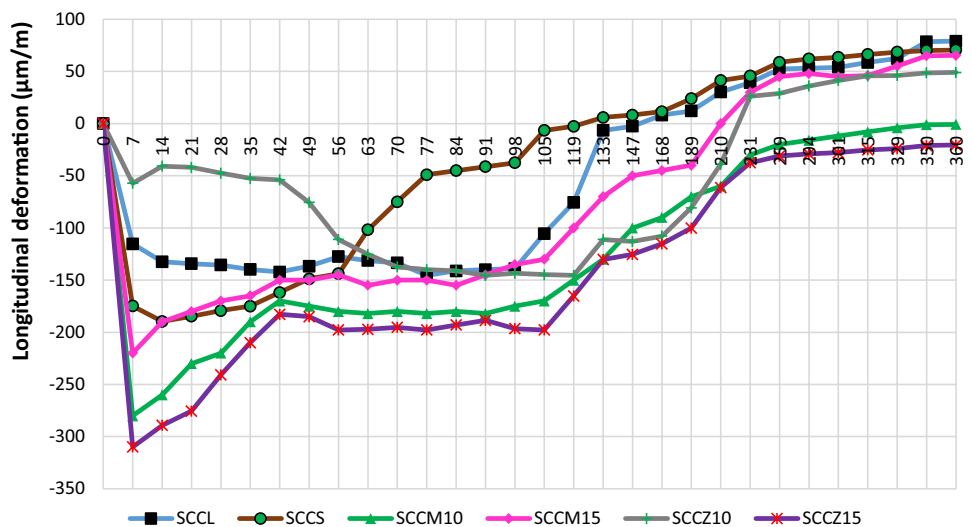
of immersion, a negligible compressive strength loss in SCC containing sand filler (SCCS) and in SCC with 10% of metakaolin (SCCM10) was observed compared to that in the initial state. Based on Fig. 12, the remarkable compressive strength loss did not occur for all mixtures at all times of immersion. On the other hand, the preservation of samples in sulfate media can reduce the rate of progression in compressive strength.

Figure 13 demonstrates the result concerning longitudinal deformations for different. In order to draw the diagram for the progress of the longitudinal deformations for all mixtures in this study, the zero point is considered as the border in the boundary between the part shrinkage and expansion. The part above the horizontal axis represents expansion, and the

**Fig.12** The change of the compressive strength of all SCCs preserved in 5% MgSO<sub>4</sub> and freshwater



**Fig.13** The results of the longitudinal deformations for all SCCs compared to the last measurement before immersion in the magnesium sulfate solution



reverse is for shrinkage. According to the result presented in Fig. 13, the expansion is recorded for all the formulations except for SCCM10 and SCCZ15 after 360 days of immersion in 5% magnesium sulfate solution. Also, from this figure, the duration of each step relating to shrinkage or expansion and the corresponding values of the deformation is different from one concrete to another. For SCCZ15, it has the most considerable shrinkage during the immersion time compared to other mixtures. Their maximum value in shrinkage is equal to  $310 \mu\text{m/m}$ . From these results, a rapid increase in shrinkage is observed in early immersion duration for all SCCs studied.

From the result illustrated in Fig. 13, the first expansion was recorded for SCCS from 133 days of immersion. Their expansion value was equal to  $5.9 \mu\text{m/m}$ . The SCCS mixture indicates a higher expansion rate than that of control mixture across the entire duration of immersion except at the end of the test. The amount of long-term expansion in SCC with limestone filler is expected to be higher compared to that in SCC containing sand filler. The reason is that the CaO quantity in limestone filler is more compared to that in sand filler. In this way, in response to the decomposition of CaO to  $\text{Ca}^{2+}$ , the possibility of gypsum production increases in

SCC with limestone filler. In this study, after 360 days of immersion, the expansion value in SCCL was almost similar to that in SCCS. We did not see higher expansion in SCCL compared to SCCS because of the limit in test duration in our work. According to the results shown in Fig. 13, before 70 days of immersion, the rate of shrinkage in SCC containing 10% zeolite was lower than that in control SCC. Then, a stable state of shrinkage was found for SCCZ10 between 70 and 98 days of immersion. According to these results, the expansion in SCCM15 and SCCZ10 at the end of the test was equal to 65 and  $48.6 \mu\text{m/m}$ , respectively. From the results shown in Fig. 13, the immersion time did not allow any expansion to be recorded for SCCM10 and SCCZ15. Accordingly, we can conclude that the incorporation of 10% metakaolin or 15% of zeolite in self-consolidating concrete among the other mixtures studied in this research is more appropriate for the character of the longitudinal deformation in external magnesium sulfate attack test.

The photographs were taken to evaluate the signs of external deterioration of concrete specimens such as alteration, cracking and spalling after 365 days of immersion in 5%  $\text{MgSO}_4$  solution (Fig. 14). Signs of spalling and white spot on surfaces were observed in all specimens. The degree

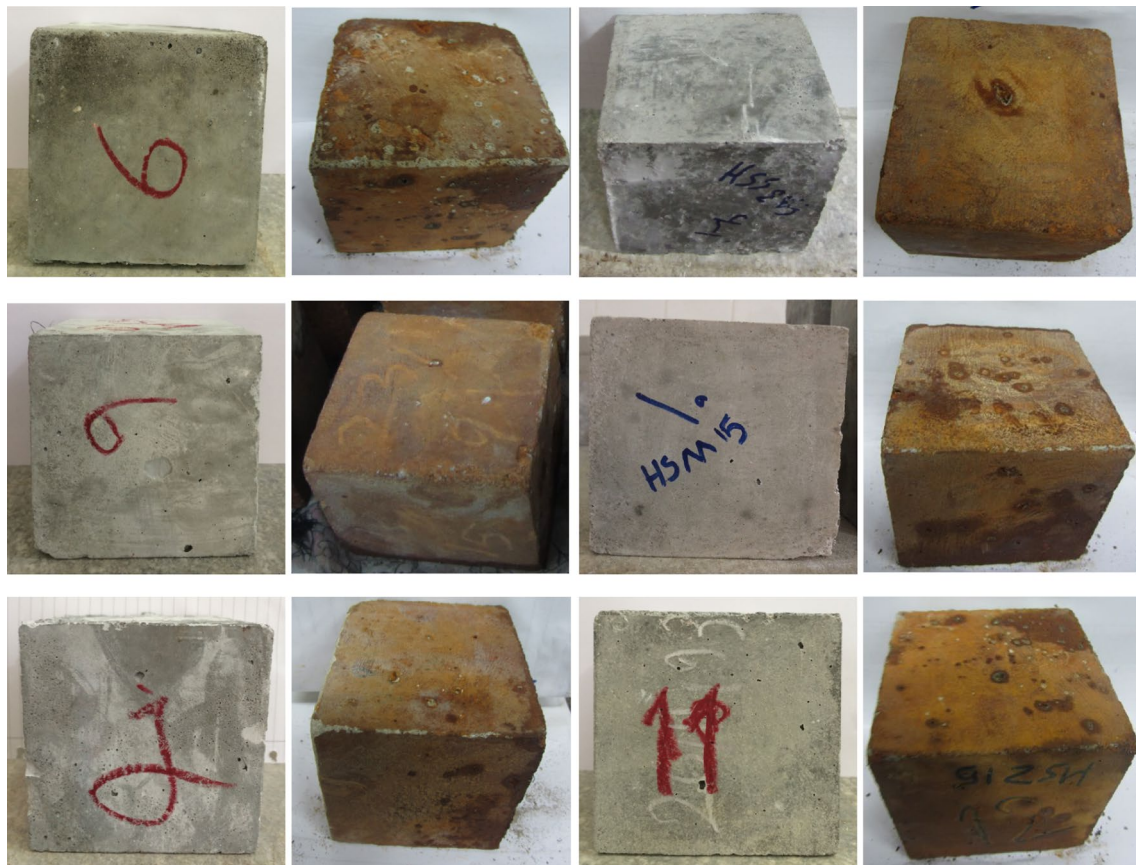


Fig. 14 Specimens before (left) and after (right) 365 days of immersion in 5%  $\text{MgSO}_4$  solution

of deterioration in SCCL appeared to be highest, with more considerable physical expansion plus a significant amount of spalling and cracking at corners and edges. Severe exterior damage was also recorded in SCCM10, SCCM15, SCCZ10 and SCCZ15. These samples more or less kept their form, with clearly deteriorated layers in exposed surfaces. Finally, the concrete with sand filler samples (SCCS) underwent minimal change, mainly on the external surfaces.

From our previous published works, the sorptivity, porosity and rate of chloride ions diffusion in SCC with sand filler are higher compared to that in SCC with limestone filler (Samimi et al. 2018b; Hocine Siad 2015). On the other hand, these elements in SCC containing metakaolin and zeolite are lower compared to that in control SCC (Samimi et al. 2017, 2018b). According to Rozière et al. (2009), diffusion is the primary mechanism of aggressive ions penetration. This hypothesis is consistent with our result when comparing control SCC and other formulations. The higher sensitivity rate in SCC with sand filler against the  $MgSO_4$  attack can be justified by their higher porosity, capillary absorption and diffusivity compared to other mixtures. In SCCS, the expansion occurs earlier than that in control SCC, because the higher porosity in SCCS leads to an enhanced diffusion of sulfate ions in concrete which promotes more massive production of gypsum. The latter is a determining agent for concrete expansion under sulfate attack. Besides, gypsum can influence on the compression strength variation of concrete studied. Therefore, the progress of compressive strength during hydration will be low.

The mass variation and degradation from visual examination in SCC containing sand filler is less than the other mixtures. On the other side, their expansion happens earlier than other SCCs. Therefore, there is no direct relationship

between mass variation, longitudinal deformation and visual examination for SCCS in our study. Also, the progress rate in compressive strength for SCCS is lower. According to the visual examination in this study, the rate of deterioration in SCC with sand filler is less than the other formulations. Conversely, the amount of expansion is higher in this one. The reason for expansion can be justified probably by the higher gypsum produced in SCCS. Accordingly, less deterioration in SCCS can be justified because the expansion in this one can happen gradually and, furthermore, the adhesion of the paste can be reduced gradually. Via a low mass gain during all the immersion period, a meager immersion expansion and the absence of compressive strength loss after 360 days, SCCs containing 15% of zeolite show good behavior compared to other formulations vis-à-vis the magnesium sulfate attack. The results obtained for the positive effect of pozzolanic admixture on the resistance of SCC exposed to  $MgSO_4$  solution agree with those of the literature (Hassan et al. 2013; Hocine Siad 2015).

#### 4.4 Chloride Ion Penetration

Figures 15, 16 and 17 show the amount of free, total and chloride binding ions, respectively, from 6 mm to every 3 mm from the depth of SCC immersed in saline solution with the concentration of 165 g/l for 90 days of the test. Due to the disruption of chloride ions, especially at the 3 mm depth, we cannot reach a decisive conclusion. This is why we have the plotted graph of total, free and bound chloride ions from 6 mm of penetration.

From the result shown in Fig. 15, free chloride ion content in many depths of SCC with sand filler and SCC containing metakaolin and zeolite is lower compared to that in control.

**Fig. 15** Content of free chloride ions per 100 g of sample (%)

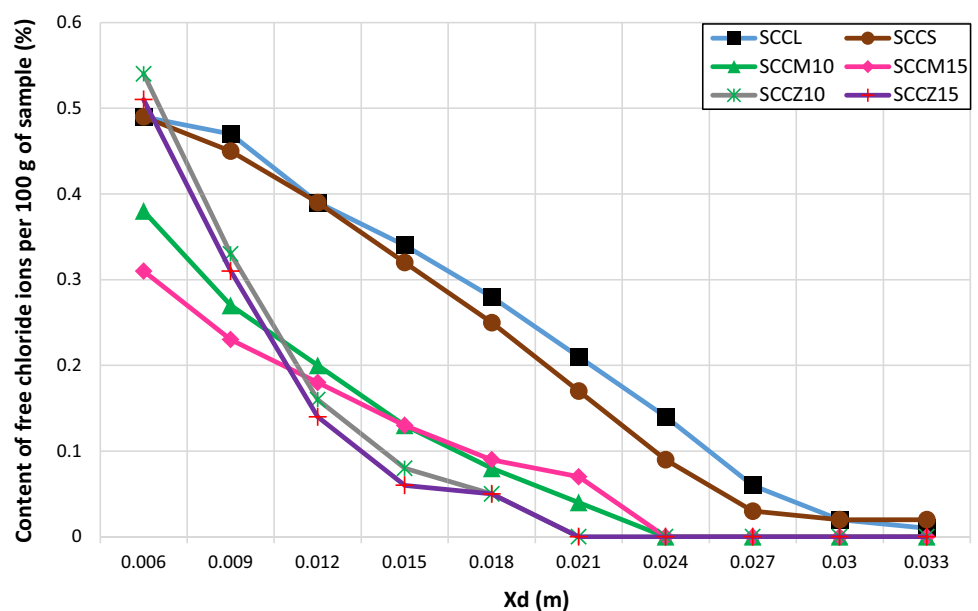


**Fig.16** Content of total chloride ions per 100 g of sample (%)

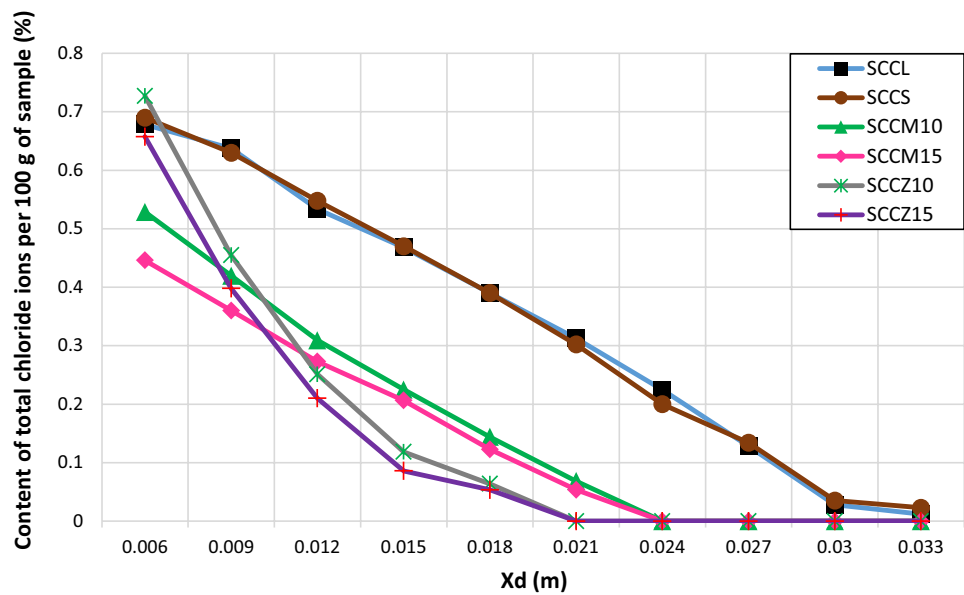
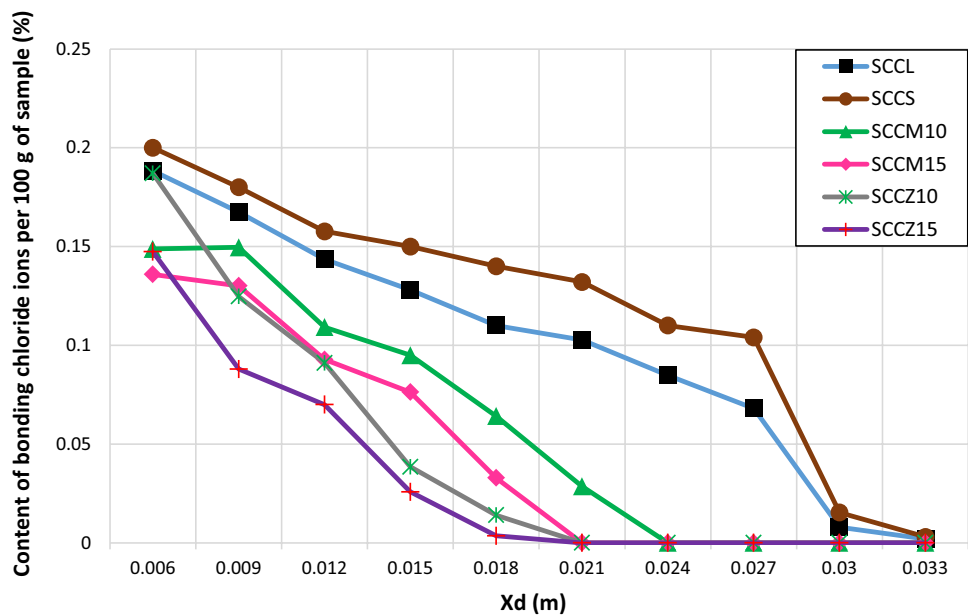


**Fig.17** Content of binding chloride ions per 100 g of sample (%)



This difference is increasingly more visible in mixtures with pozzolan. Also, the content of free chloride ions in many depths of SCC decreases by increasing the percentage of pozzolan. From Fig. 16, the content of total chloride ions in many depths of SCC with sand filler is almost identical with that in control SCC. From these results, the content of total chloride ions in SCC containing pozzolan shows the same tendency as illustrated in the diagram of free chloride ion content. From the result shown in Fig. 17, the content of chloride ion binding in all penetration depths of SCC with sand filler is more significant compared to that in control SCC. According to this figure, the content of chloride ions binding in SCC containing pozzolan shows the same

tendency as illustrated in the diagram concerning the content of free and total chloride ions. Also, the content of bounding chloride ions in SCC containing metakaolin or zeolite decreases by increasing the percentage of substitution. According to Nguyen et al. (2006), the content of bounding chloride ions in the mixture containing additive is higher compared to that in mixture without additives. In this way, according to him, the bounding chloride ion content is more excellent for mixtures which have the lower free chloride ion content. It should be noted that the type of chloride penetration in their study was steady-state migration which is utterly different from the procedure carried out in our study. On the other hand, since the aluminate phase has a determining

role on the higher bounding chloride ion level, the theory proposed by Nguyen et al. (2006) may be applicable where the amount of aluminate phase existing in the cement paste is at the higher level. In this study, this theory is entirely in agreement for SCC containing sand filler. By considering that the  $C_3A$  phase in cement paste existing in SCCS is constant compared to that in control SCC, the amount of  $Al_2O_3$  in sand filler and limestone filler is equal to 14.42 and 0.85, respectively (Table 1). Therefore, the difference in the amount of  $Al_2O_3$  between sand filler and limestone filler is remarkable. In this manner, the higher amount of bounding chloride ions in SCCS compared to that in control SCC is reasonable. However, the amount of aluminate ( $Al_2O_3$ ) existing in metakaolin and zeolite is low, 13.71% and 13.54%, respectively (Table 1). Therefore, the theory mentioned by Nguyen et al. (2006) has not been observed using the low level of aluminate existing in metakaolin and zeolite used in this study. Also, the less content of chloride binding in mixture containing pozzolan compared to the control mixture is explained by the following two reasons:

1. The aluminate phase presented to the mixture containing pozzolan decreased because the level of  $C_3A$  existing in clinker of cement paste decreases by replacing pozzolan. On the other hand, the pozzolans used in this study are not able to compensate for the lack of aluminate phase due to the low level of aluminate existing in our pozzolan. In this way, the alkalinity of pore solution decreases in the mixture containing pozzolan and, consequently, the product of Friedel salt and thus the bounding chloride decreases.
2. The physical fixation capacity of chloride in concrete depends on the  $CaO/SiO_2$  ratio. A low  $CaO/SiO_2$  ratio leads to low chloride fixation because the positive charge

on the pore surface is small, which reduces the adsorption of negative ions (Beaudoin et al. 1990; Maes et al. 2013; Khoshroo et al. 2018b). The mentioned ratio may be smaller in the mixture studied based on pozzolan than in those made without additives. This leads to lower physical fixation of chlorides in the mixture based on pozzolan. These results relating to bounding chloride ions obtained for mixture based on pozzolan in this study are in complete agreement with the result from Nguyen et al. (2006) for mixtures based on CEM V.

Figure 18 shows the relationship between chloride binding and free chloride percent of mixtures. As it is clear from the figure, there is no direct relation between these two parameters. Therefore, it seems that other criteria such as microstructural parameters affect the results. Also, the relationship between the mass variation immersed in the  $MgSO_4$  solution and compressive strength of mixtures is shown in Fig. 19. It is evident that we can consider a good polynomial-type relation between these two parameters.

## 5 Conclusion

This study attempts to answer several questions concerning the influence of sand filler and two pozzolans such as metakaolin and zeolite by incorporating them in the self-consolidating concrete vis-à-vis attacks by a rich medium of  $MgSO_4$  and chloride. The results of the research are summarized as below:

1. The mineralogical analyses, as well as pozzolanic activity, showed that zeolite studied is a clinoptilolite having

**Fig. 18** Relationship between the chloride binding and free chloride ions

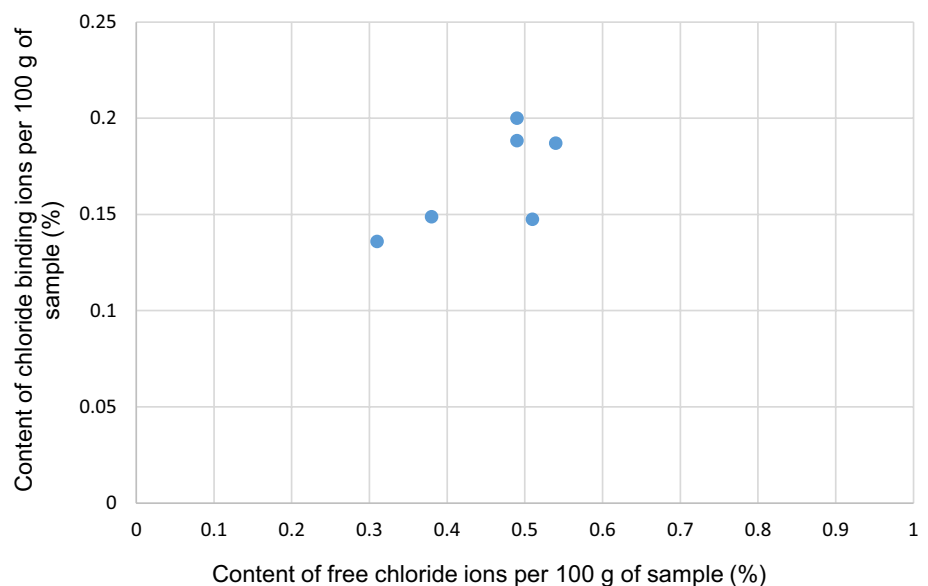
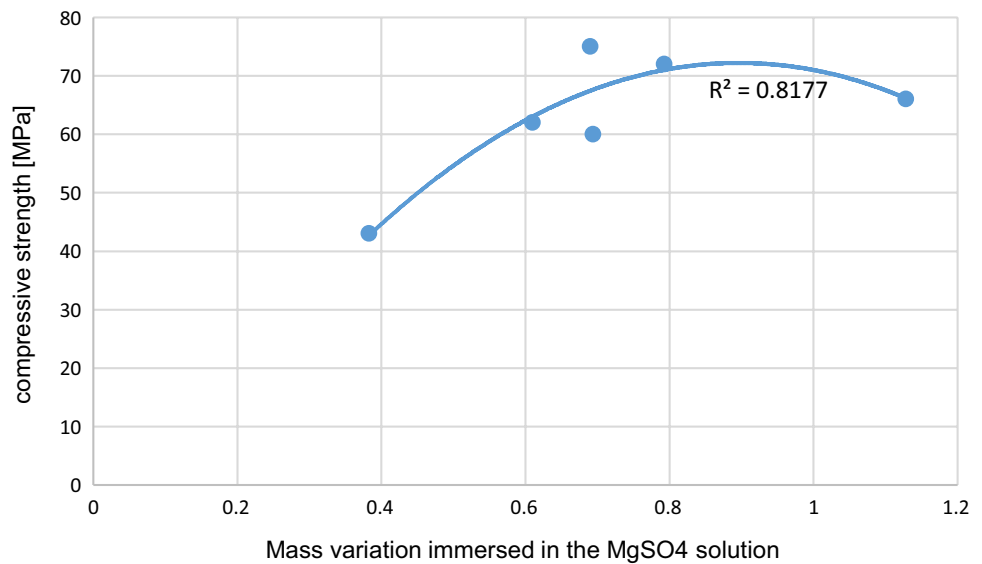


**Fig.19** Relationship between mass variation immersed in the  $\text{MgSO}_4$  solution and compressive strength



- an activity superior to that of metakaolin pozzolan. XRD diffractogram of metakaolin showed that it is composed of anorthite and quartz minerals which are siliceous metakaolins.
2. SCCZ10 and SCCZ15, despite the strong pozzolanic activity of zeolite, show a low compressive strength compared to the control SCC. On the other hand, mixtures containing metakaolin have the best compressive strength compared to the control mixture. A significant increase in compressive strength is observed at early age and in the long term for SCC containing 15% of metakaolin. The compressive strength results are in complete agreement with the results from the thermal analysis.
  3. The reaction of magnesium sulfate attack is prolonged and may take many years before a characteristic degradation. The control SCC systematically has the most significant mass gain compared to other formulations.
  4. The compressive strength loss because of  $\text{MgSO}_4$  attack is observed compared to their initial value for SCCS and SCCM10 at the age of 28 days of immersion. On the other hand, it is not found until the end of the immersion test time.
  5. The comparison between the control condition and the sulfate condition confirmed the rate of degradation by the external attack of magnesium sulfate. This fact can show the influence of sulfate attack by producing gypsum, filling micro-cracks by water and the participation of water in relative reaction to produce secondary ettringite. The expansion in all formulations is visible at the end of test time except in SCCM10 and SCCZ15.
  6. By a low growth in mass during all the immersion period, a meager immersion expansion and the absence of compressive strength loss after 360 days, the SCC containing 15% zeolite shows the best physicochemical

and mechanical resistance compared to other mixtures vis-à-vis the  $\text{MgSO}_4$  attack.

7. The positive effect of zeolite on the chloride ions penetration is related to the reactivity of this pozzolan and consequently the consumption of calcium hydroxide, which leads to very probably an increase in tortuosity and a reduction of  $\text{OH}^-$  ions in the interstitial solution. As a result, the conductivity and penetration of chloride ions will decrease.

## References

- Alanazi H, Yang M, Zhang D, Gao Z (2017) Early strength and durability of metakaolin-based geopolymer concrete. *Mag Concr Res* 69(1):46–54
- Anissa Bessa J-PB-L (2004) Evaluation de la contribution liante des additions minérales à la porosité, à la résistance en compression et la durabilité des mortiers. XXIIèmes Rencontres Universitaires de Génie Civil- Ville & Génie Civil
- Beaudoin JJ, Ramachandran VS, Feldman RF (1990) Interaction of chloride and C–S–H. *Cem Concr Res* 20(6):875–883
- Behfarnia K, Farshadfar O (2013) The effects of pozzolanic binders and polypropylene fibers on durability of SCC to magnesium sulfate attack. *Constr Build Mater* 38:64–71. <https://doi.org/10.1016/j.conbuildmat.2012.08.035>
- Dousti A, Rashednia R, Ahmadi B, Shekarchi M (2013) Influence of exposure temperature on chloride diffusion in concretes incorporating silica fume or natural zeolite. *Constr Build Mater* 49:393–399. <https://doi.org/10.1016/j.conbuildmat.2013.08.086>
- Ghrici M, Kenai S, Said-Mansour M (2007) Mechanical properties and durability of mortar and concrete containing natural pozzolana and limestone blended cements. *Cem Concr Compos* 29:542–549
- Hassan AA, Lachemi M, Hossain KM (2012) Effect of metakaolin and silica fume on the durability of self-consolidating concrete. *Cem Concr Compos* 34(6):801–807
- Hassan A, Bin Mahmud H, Jumaat MZ, Alsubari B, Abdulla A (2013) Effect of magnesium sulfate on self-consolidating concrete

- containing supplementary cementitious materials. *Adv Mater Sci Eng* 2013:1–8
- Hocine Siad ML (2015) Assessment of the long-term performance of SCC incorporating different mineral admixtures in a magnesium sulfate environment. *Constr Build Mater* 80:141–154
- Karakurt C, Topçu İB (2011) Effect of blended cements produced with natural zeolite and industrial by-products on alkali-silica reaction and sulfate resistance of concrete. *Constr Build Mater* 25(4):1789–1795. <https://doi.org/10.1016/j.conbuildmat.2010.11.087>
- Khoshroo M, Javid S, Akbar A, Katebi A (2018a) Effects of micro-nano bubble water and binary mineral admixtures on the mechanical and durability properties of concrete. *Constr Build Mater*. <https://doi.org/10.1016/j.conbuildmat.2017.12.225>
- Khoshroo M, Javid AAS, Katebi A (2018b) Effect of chloride treatment curing condition on the mechanical properties and durability of concrete containing zeolite and micro-nano bubble water. *Constr Build Mater* 177:417–427. <https://doi.org/10.1016/j.conbuildmat.2018.05.086>
- Maes M, Gruyaert E, De Belie N (2013) Resistance of concrete with blast-furnace slag against chlorides, investigated by comparing chloride profiles after migration and diffusion. *Mater Struct* 46(1–2):89–103
- Maes M, Mittermayr F, De Belie N (2017) The influence of sodium and magnesium sulfate on the penetration of chlorides in mortar. *Mater Struct* 50(2):153
- Najimia M, Sobhani J, Ahmadi B, Shekarchi M (2012) An experimental study on durability properties of concrete containing zeolite as a highly reactive natural pozzolan. *Constr Build Mater* 35:1023–1033. <https://doi.org/10.1016/j.conbuildmat.2012.04.038>
- Neville A (2004) The confused world of sulfate attack on concrete. *Cem Concr Res* 34(8):1275–1296
- NF P18-513 (2012) Détermination de la quantité d'hydroxide de calcium fixé. Essai chapelle modifié
- Nguyen VH, Nedjar B, Colina H, Torrenti JM (2006) A separation of scales analysis for the modelling of calcium leaching in concrete. *Comput Methods Appl Mech Eng* 195:7196–7210
- Rozière E, Loukili A, El Hachem R, Grondin F (2009) Durability of concrete exposed to leaching and external sulfate attacks. *Cem Concr Res* 39(12):1188–1198
- Sabet FA, Libre NA, Shekarchi M (2013) Mechanical and durability properties of self-consolidating high performance concrete incorporating natural zeolite, silica fume and fly ash. *Constr Build Mater* 44:175–184. <https://doi.org/10.1016/j.conbuildmat.2013.02.069>
- Samimi K, Kamali-Bernard S, Maghsoudi AA, Maghsoudi M, Siad H (2017) Influence of pumice and zeolite on compressive strength, transport properties and resistance to chloride penetration of high strength self-compacting concretes. *Constr Build Mater* 151:292–311
- Samimi K, Kamali-Bernard S, Maghsoudi AA (2018a) Durability of self-compacting concrete containing pumice and zeolite against acid attack, carbonation and marine environment. *Constr Build Mater* 165:247–263
- Samimi K, Kamaragi D, Roy L (2018b) Microstructure, thermal analysis and chloride penetration by different condition of self-compacting concrete. *Mag Concr Res*. <https://doi.org/10.1680/jmacr.17.00367>
- San Nicolas R, Cyr M, Escadeillas G (2014) Performance-based approach to durability of concrete containing flash-calcined metakaolin as cement replacement. *Constr Build Mater* 55:313–322
- Santhanam M (2001) Studies on sulfate attack – mechanisms, test methods and modeling. PhD Dissertation Purdue University, West Lafayette, Indiana, USA
- Siddique R, Klaus J (2009) Influence of metakaolin on the properties of mortar and concrete: a review. *Appl Clay Sci* 43(3):392–400
- Tadayon MH, Shekarchi M, Tadayon M (2016) Long-term field study of chloride ingress in concretes containing pozzolans exposed to severe marine tidal zone. *Constr Build Mater* 123:611–616. <https://doi.org/10.1016/j.conbuildmat.2016.07.074>
- Tagnit-Hamou A, Petrov N (2000) Durability of concrete in a Very Aggressive Environment. In: Proceedings of the international conference on cement microscopy. International Cement Microscopy Association, pp 420–430.
- Tosun K, Felekoglu B, Baradan B, Altun IA (2009) Effects of limestone replacement ratio on the sulfate resistance of Portland limestone cement mortars exposed to extraordinary high sulfate concentrations. *Constr Build Mater* 23:2534–2544
- Valipour M, Pargar F, Shekarchi M, Khani S (2013) Comparing a natural pozzolan, zeolite, to metakaolin and silica fume in terms of their effect on the durability characteristics of concrete: a laboratory study. *Constr Build Mater* 41:879–888. <https://doi.org/10.1016/j.conbuildmat.2012.11.054>
- Valipour M, Shekarchi M, Arezoumandi M (2017) Chlorine diffusion resistivity of sustainable green concrete in harsh marine environments. *J Clean Prod* 142(Part 4):4092–4100. <https://doi.org/10.1016/j.jclepro.2016.10.015>
- Zhang Y, Zhang M, Ye G (2018) Influence of moisture condition on chloride diffusion in partially saturated ordinary Portland cement mortar. *Mater Struct* 51(2):36